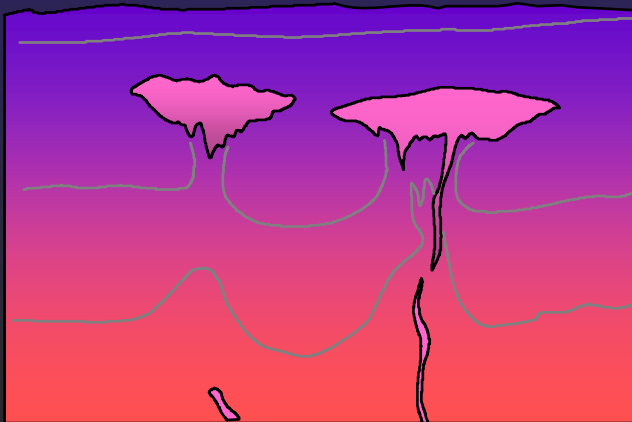


Origin of Basaltic Magma



Geology 323- Petrology

2 principal types of basalt in the ocean basins

Tholeiitic Basalt and Alkaline Basalt

Table 10-1 Common petrographic differences between tholeiitic and alkaline basalts

| | Tholeiitic Basalt | Alkaline Basalt |
|--------------------|---|---|
| Groundmass | <p>Usually fine-grained, intergranular</p> <p>No olivine</p> <p>Clinopyroxene = augite</p> <p>Orthopyroxene (hypersthene) common</p> <p>No alkali feldspar</p> <p>Interstitial glass and/or quartz common</p> | <p>Usually fairly coarse, intergranular to ophitic</p> <p>Olivine common</p> <p>Titaniferous augite</p> <p>Orthopyroxene absent</p> <p>Interstitial alkali feldspar or feldspathoid may occur</p> <p>Interstitial glass rare, and quartz absent</p> |
| Phenocrysts | <p>Olivine rare, unzoned, and may be partially resorbed or show reaction rims of orthopyroxene</p> <p>Orthopyroxene uncommon</p> <p>Early plagioclase common</p> <p>Clinopyroxene is pale brown augite</p> | <p>Olivine common and zoned</p> <p>Orthopyroxene absent</p> <p>Plagioclase less common, and later in sequence</p> <p>Clinopyroxene is titaniferous augite, reddish rims</p> |

Each is chemically distinct

Evolve by fractional crystallization
as separate series along different
paths

- Tholeiites are generated at mid-ocean ridges
 - ✦ Also generated at oceanic islands, subduction zones
- Alkaline basalts generated at ocean islands
 - ✦ Also at subduction zones

Sources of mantle material

- Ophiolites
 - ✦ Slabs of oceanic crust and upper mantle
 - ✦ Thrust at subduction zones onto edge of continent
- Dredge samples from oceanic fracture zones
- Nodules and xenoliths in some basalts
- Kimberlite xenoliths
 - ✦ Diamond-bearing pipes blasted up from the mantle carrying numerous xenoliths from depth

Lherzolite: A type of peridotite with Olivine > Opx + Cpx

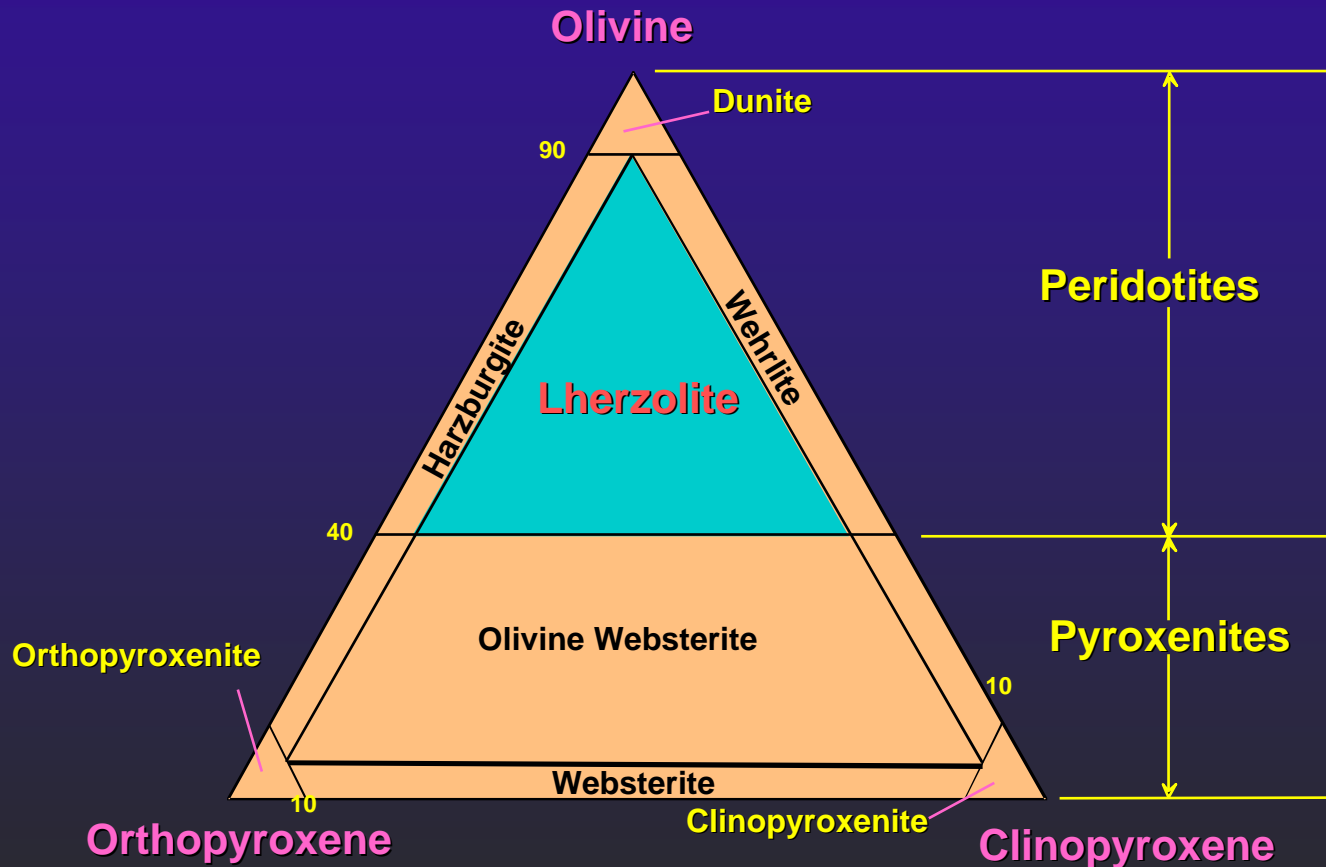


Figure 2-2 C After IUGS

Lherzolite is probably fertile unaltered mantle

Dunite and harzburgite are refractory residuum after basalt has been extracted by partial melting

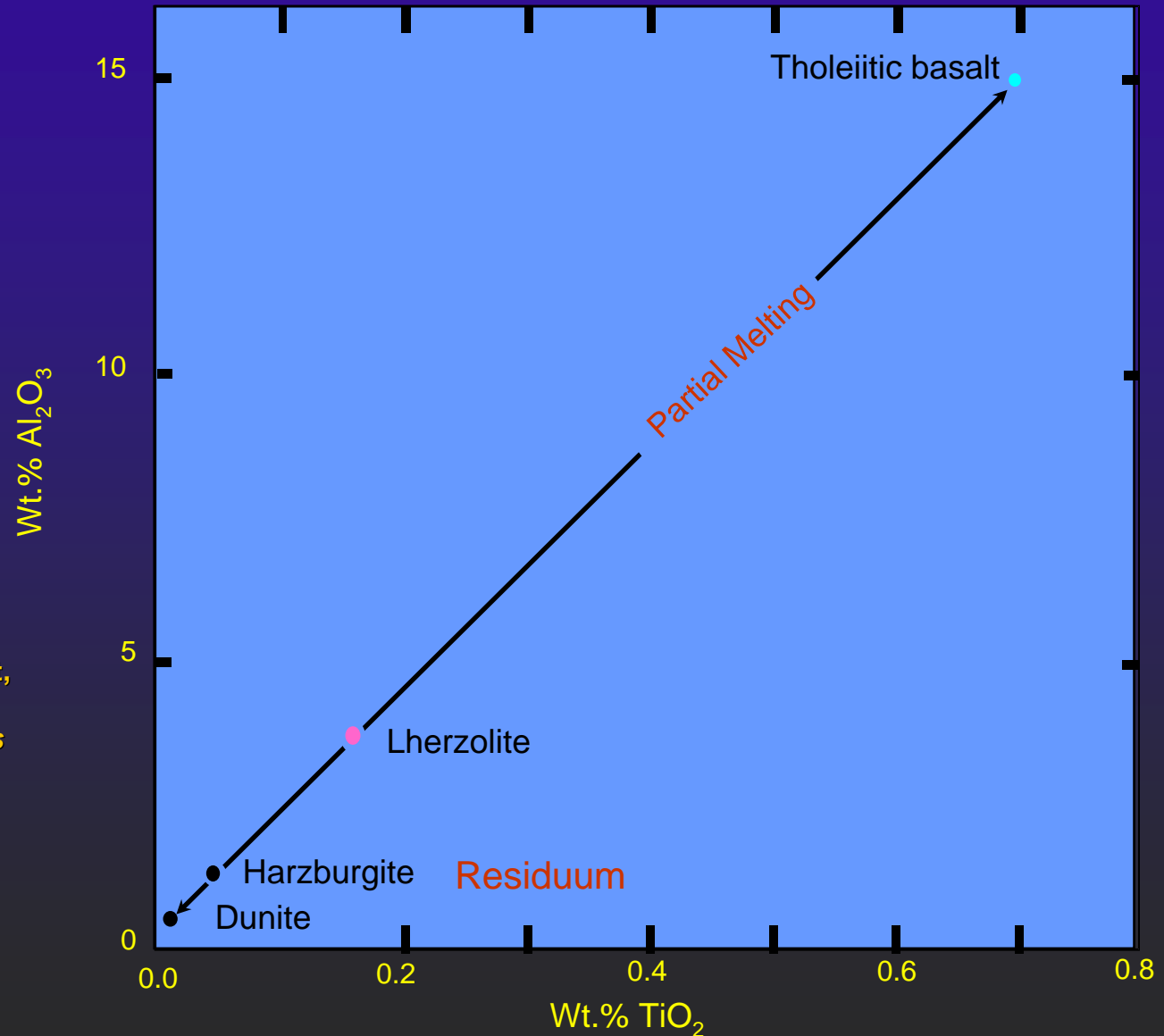


Figure 10-1 Brown and Mussett, A. E. (1993), *The Inaccessible Earth: An Integrated View of Its Structure and Composition*. Chapman & Hall/Kluwer.

Phase diagram for lherzolite with

Al-rich phase:

Al-phase =

- Plagioclase

- ◆ shallow (< 50 km)

- Spinel

- ◆ 50-80 km

- Garnet

- ◆ 80-400 km

- Si → 6-fold coordination

- ◆ > 400 km

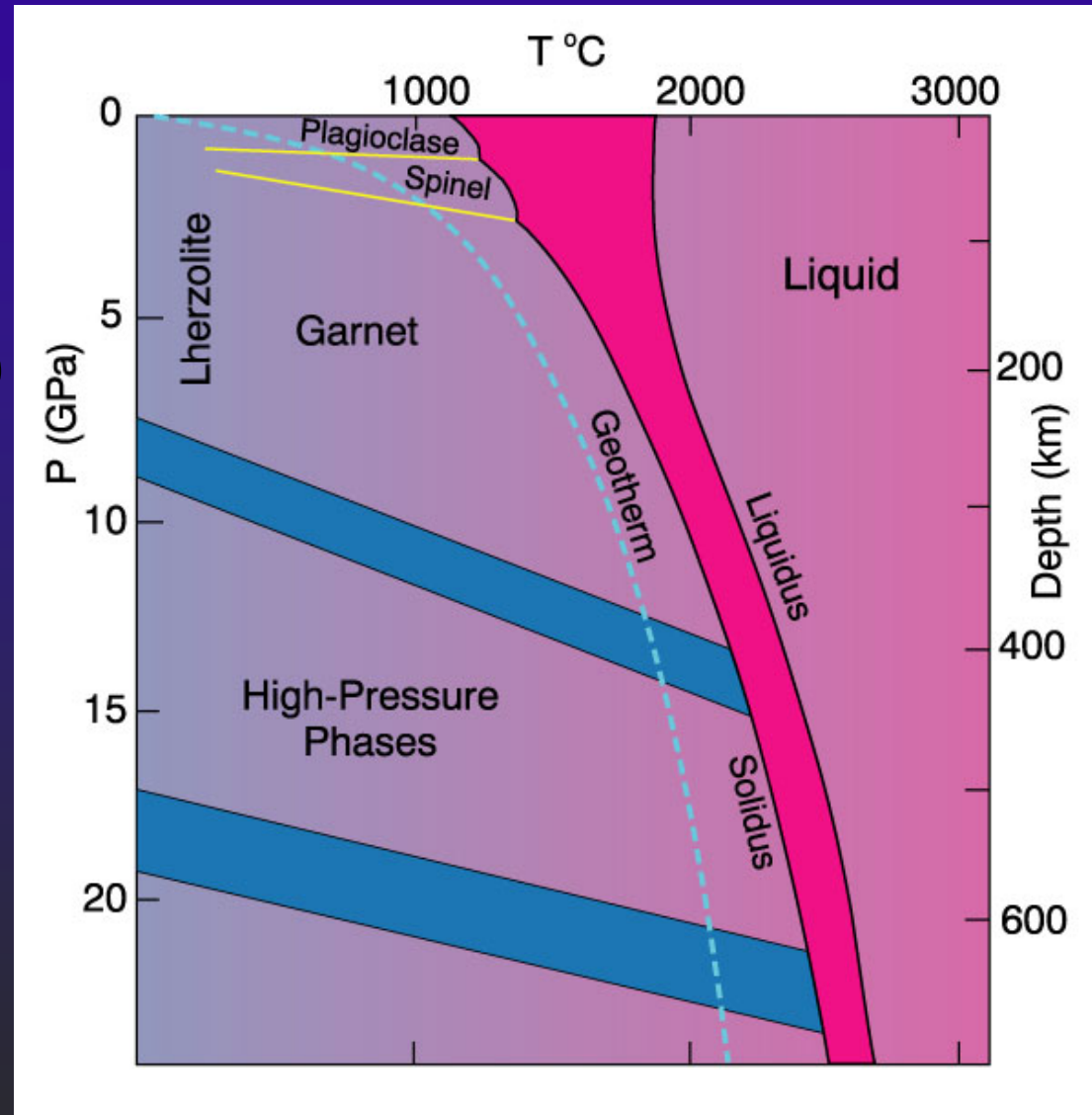


Figure 10-2 Phase diagram of aluminous lherzolite with melting interval (gray), sub-solidus reactions, and geothermal gradient. After Wyllie, P. J. (1981). Geol. Rundsch. 70, 128-153.

How does the mantle melt?

1) Increase the temperature

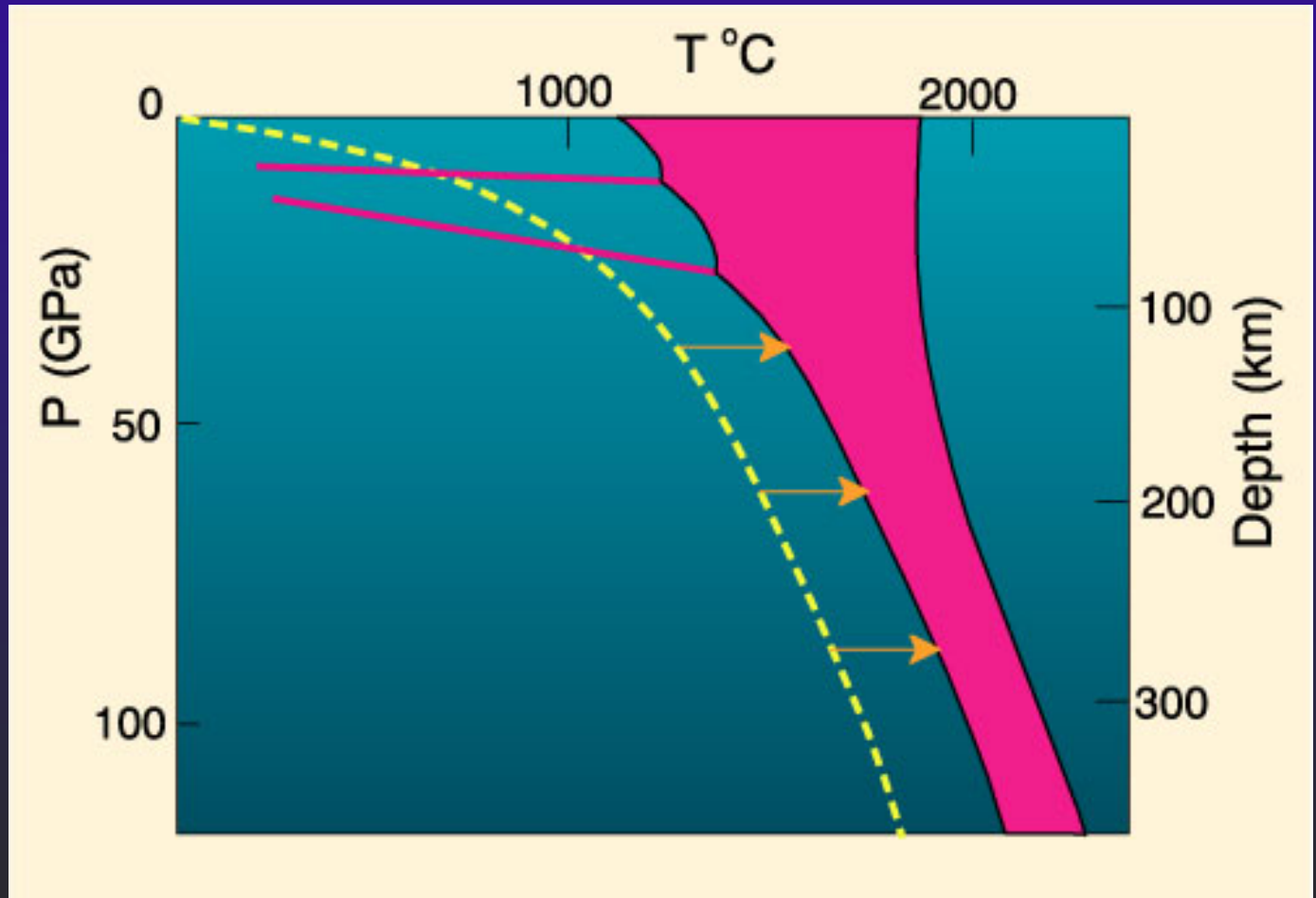


Figure 10-3. Melting by raising the temperature.

2) Lower the pressure

- ✦ Adiabatic rise of mantle with no conductive heat loss
- ✦ Decompression melting could melt at least 30%

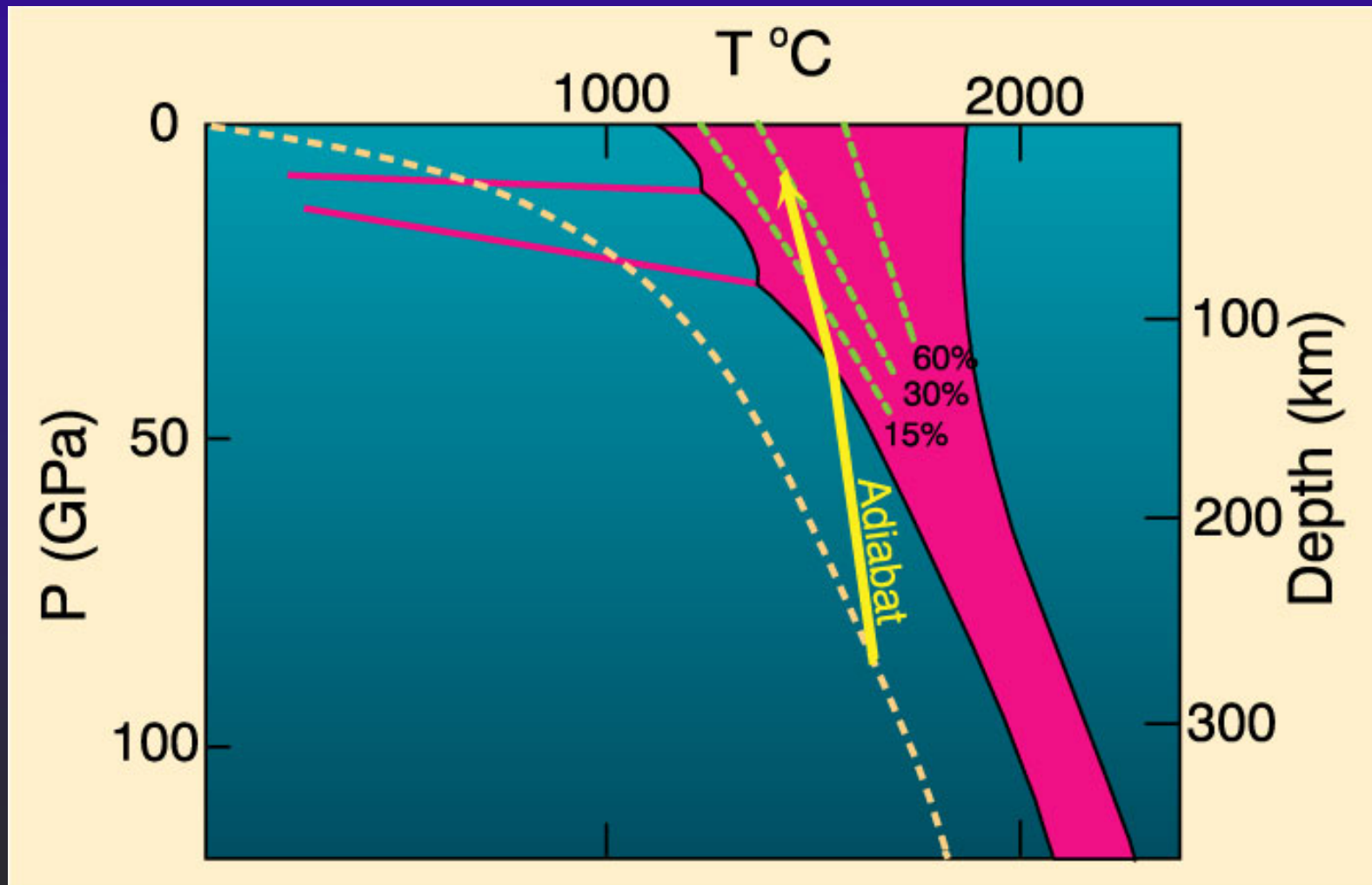


Figure 10-4. Melting by (adiabatic) pressure reduction. Melting begins when the adiabat crosses the solidus and traverses the shaded melting interval. Dashed lines represent approximate % melting.

3) Add volatiles (especially H₂O)

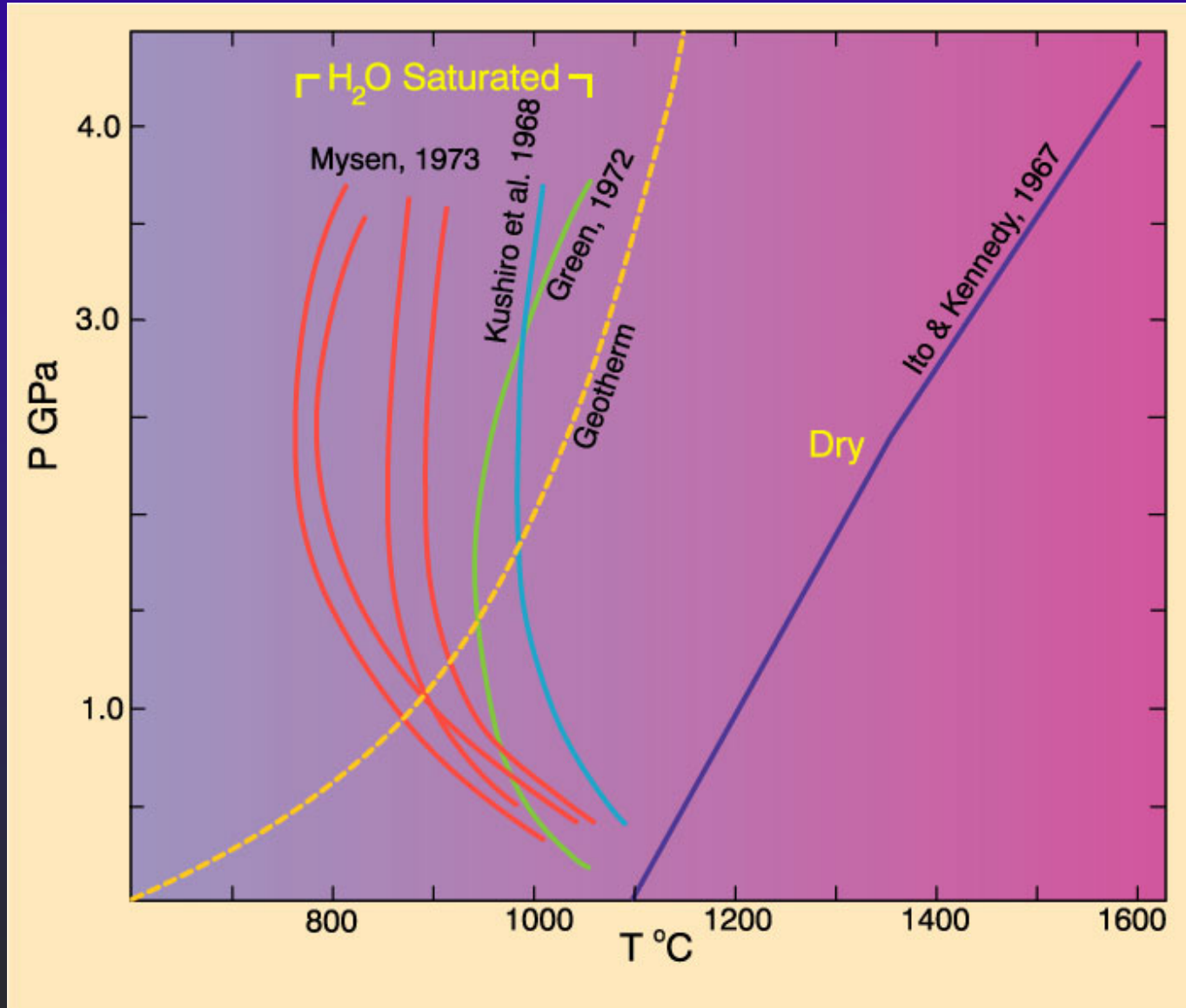


Figure 10-4. Dry peridotite solidus compared to several experiments on H₂O-saturated peridotites.

Melts can be created under realistic circumstances

- Plates separate and mantle rises at mid-ocean ridges
 - ◆ Adiabatic rise → decompression melting
- Hot spots → localized plumes of melt
- Addition of fluids may cause low velocity layer – LVL – in the asthenosphere
 - ◆ Also important in subduction zones and other settings

Generation of tholeiitic and alkaline basalts

1) Chemically uniform mantle

Variables:

Temperature

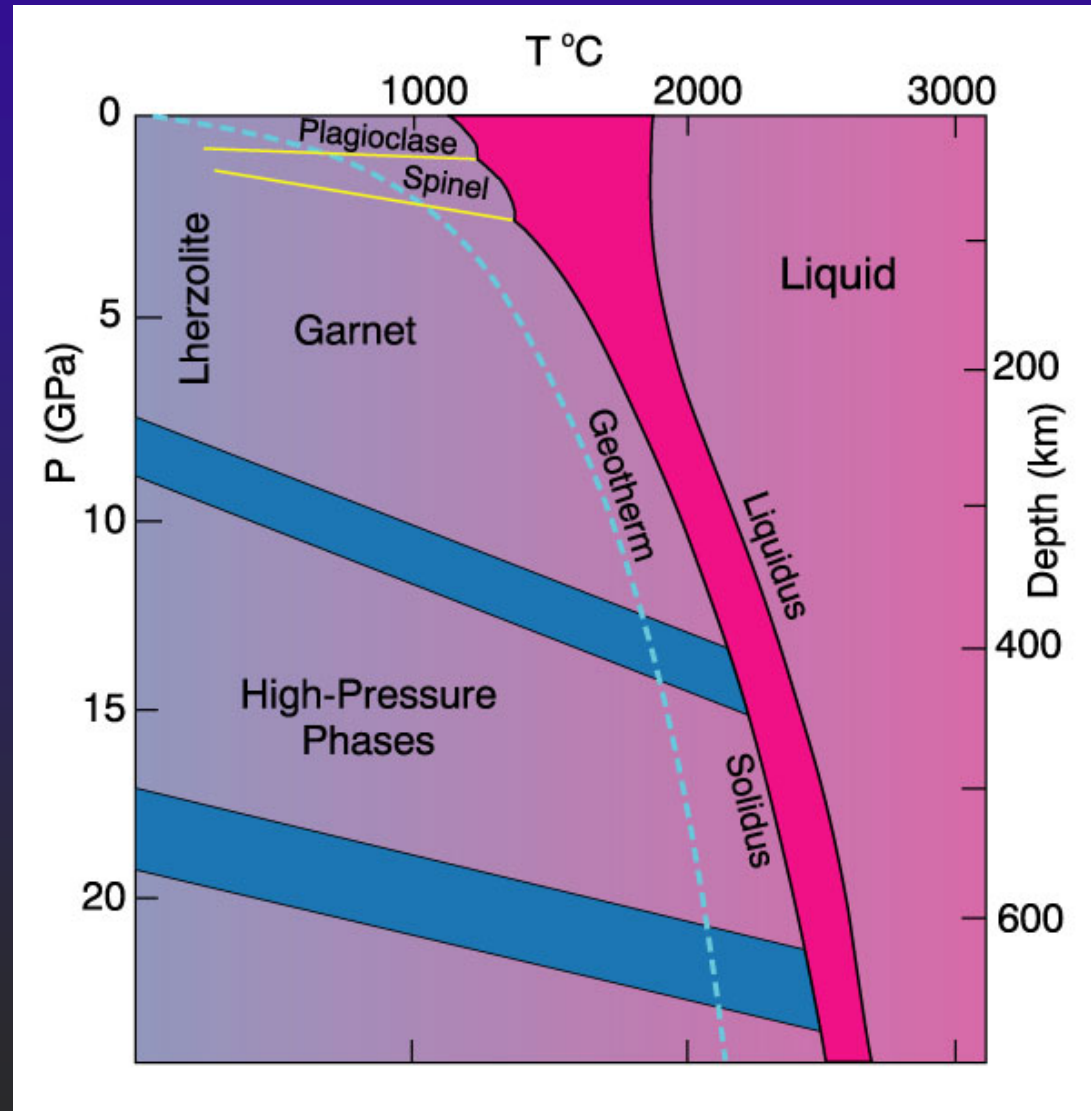


Figure 10-2 Phase diagram of aluminous lherzolite with melting interval (gray), sub-solidus reactions, and geothermal gradient. After Wyllie, P. J. (1981). Geol. Rundsch. 70, 128-153.

Variables: Pressure

Change in first melt composition (eutectic) with increasing P

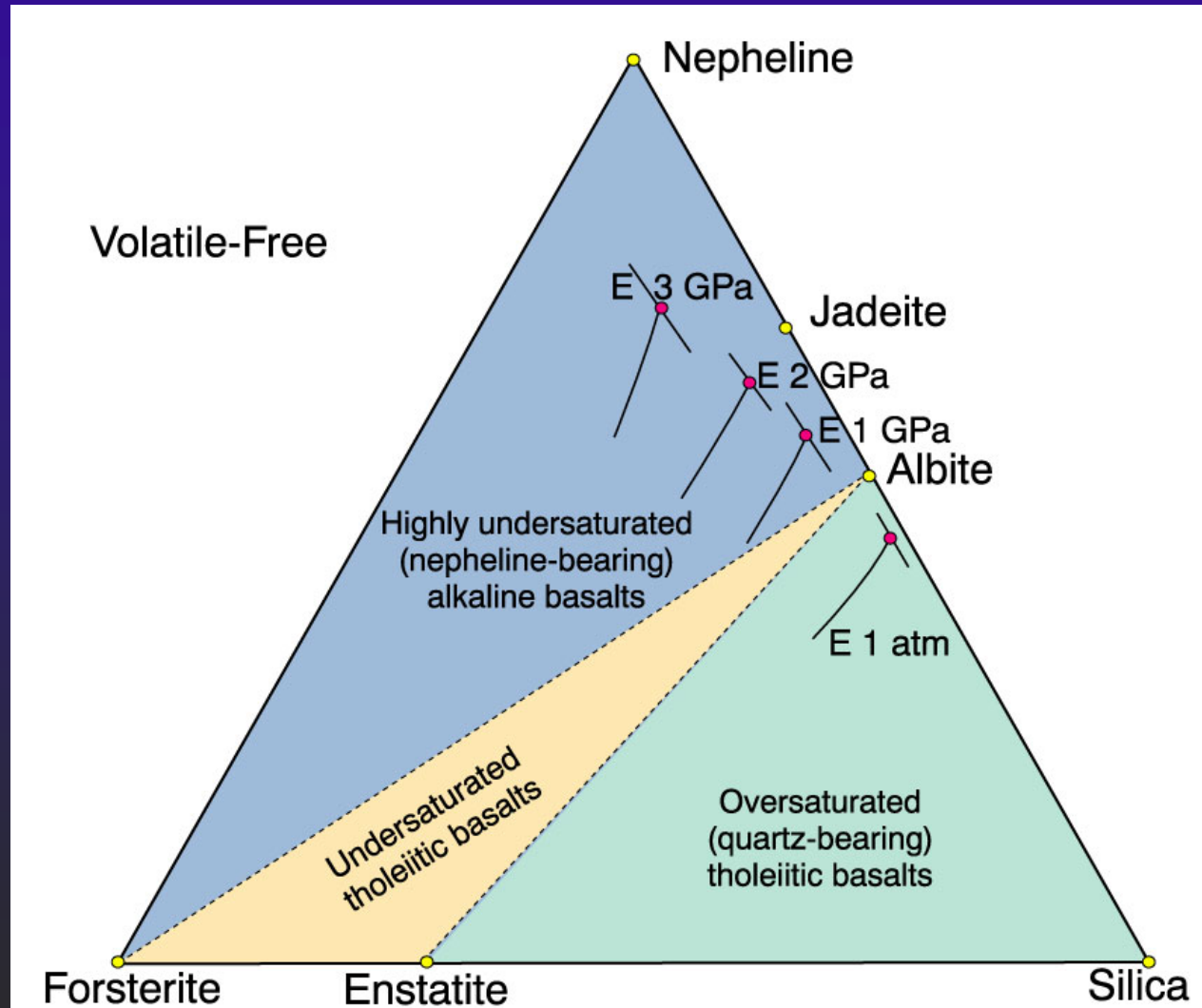


Figure 10-8 Change in the eutectic (first melt) composition with increasing pressure from 1 to 3 GPa projected onto the base of the basalt tetrahedron. After Kushiro (1968), *J. Geophys. Res.*, 73, 619-634.

Initial Conclusions:

- Tholeiites favored by shallower melting
25% melting at <30 km → tholeiite
1 GPa = 35 km depth
- Tholeiites favored by greater % partial melting
20 % melting at 60 km → alkaline basalt
30 % melting at 60 km → tholeiite

Crystal fractionation of magmas as they rise from depth

- Tholeiite → alkaline basalt by fractional crystallization at med to high P (~1.5 GPa)
- Not at low P (<1.5 GPa)
- At high P (>2 GPa)
- Low-P fractional crystallization → high-Al basalt

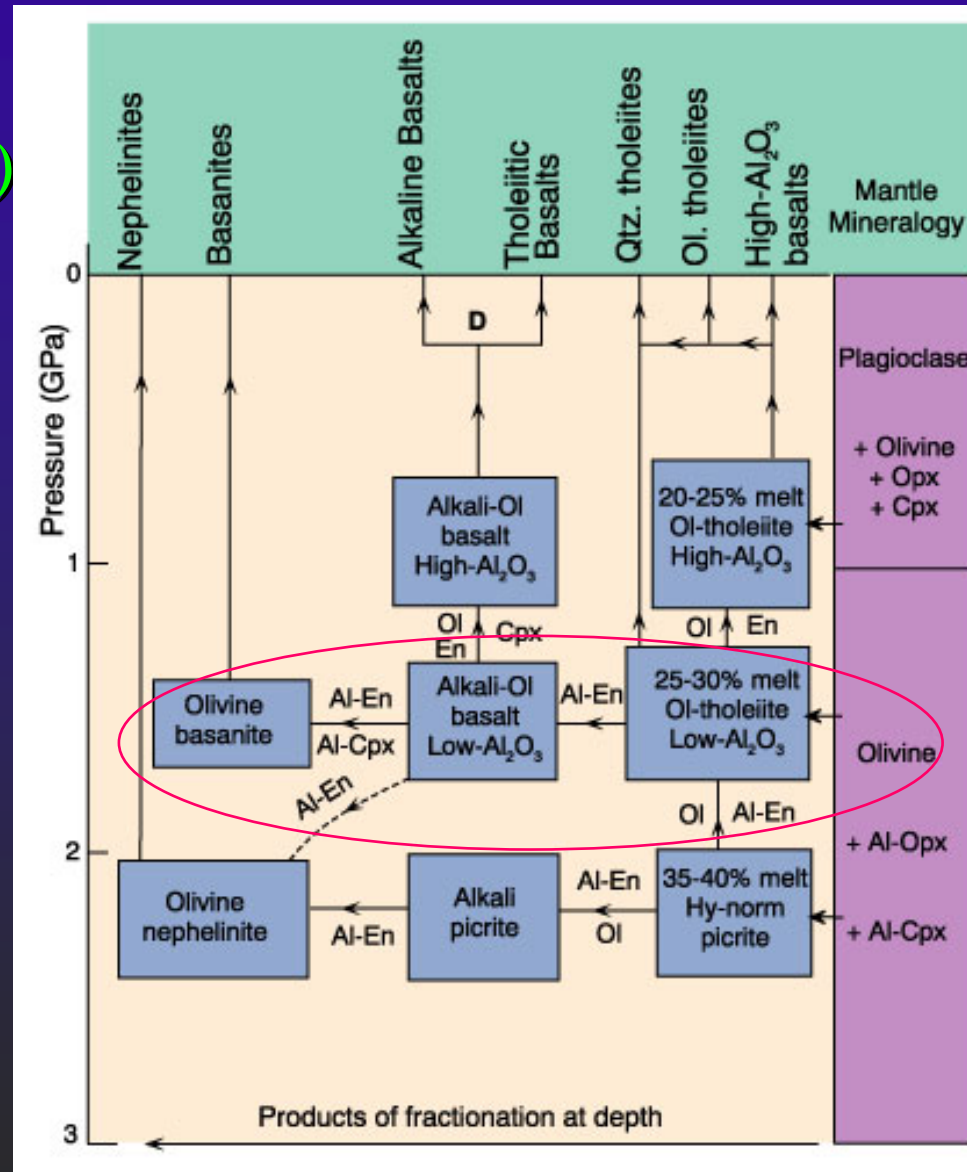


Figure 10-10 Schematic representation of the fractional crystallization scheme of Green and Ringwood (1967) and Green (1969). After Wyllie (1971). *The Dynamic Earth: Textbook in Geosciences*. John Wiley & Sons.

Models for Basalt Genesis

1. Composition of primary basalts controlled by
 - depth
 - % of partial melting
 - type of volatiles (i.e., H₂O-rich or CO₂-rich)
2. Compositions of basalt at surface controlled by fractional crystallization during ascent
3. Tholeiites = shallow melting, greater % partial melting, ol fractionation, H₂O-rich volatiles
4. Alkaline basalts = deeper sources, small % partial melting, CO₂-rich volatiles

5. Tholeiites also form by ol fractionation during rise of ol-rich basalts (picrites)
6. Alkaline basalts by deep-seated fractionation of Al-rich silicate phases (e.g., opx, cpx)

Primary magmas

- Formed at depth and not subsequently modified by fractional crystallization or assimilation

- Criteria

Highest Mg# ($100\text{Mg}/(\text{Mg}+\text{Fe})$) → parental magma

Experimental results of lherzolite melts

- ▲ Mg# = 66-75

- ▲ Cr > 1000 ppm

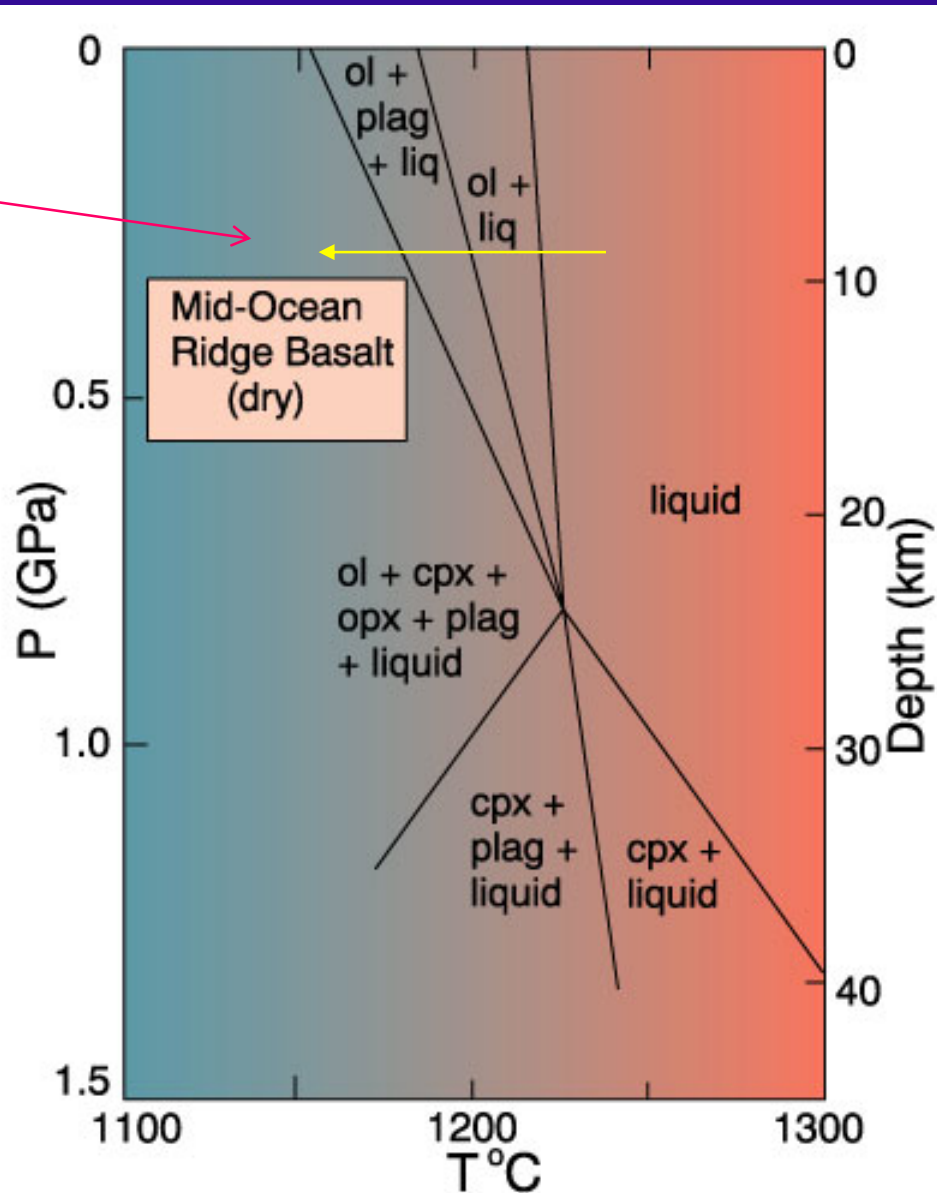
- ▲ Ni > 400-500 ppm

- ▲ Multiply saturated with different mineral phases

Multiple saturation with several mineral phases

- At Low P
Ol then Plag then Cpx as
magma cools

Figure 10-12 Anhydrous P-T phase relationships for a mid-ocean ridge basalt suspected of being a primary magma. After Fujii and Kushiro (1977). *Carnegie Inst. Wash. Yearb.*, 76, 461-465.

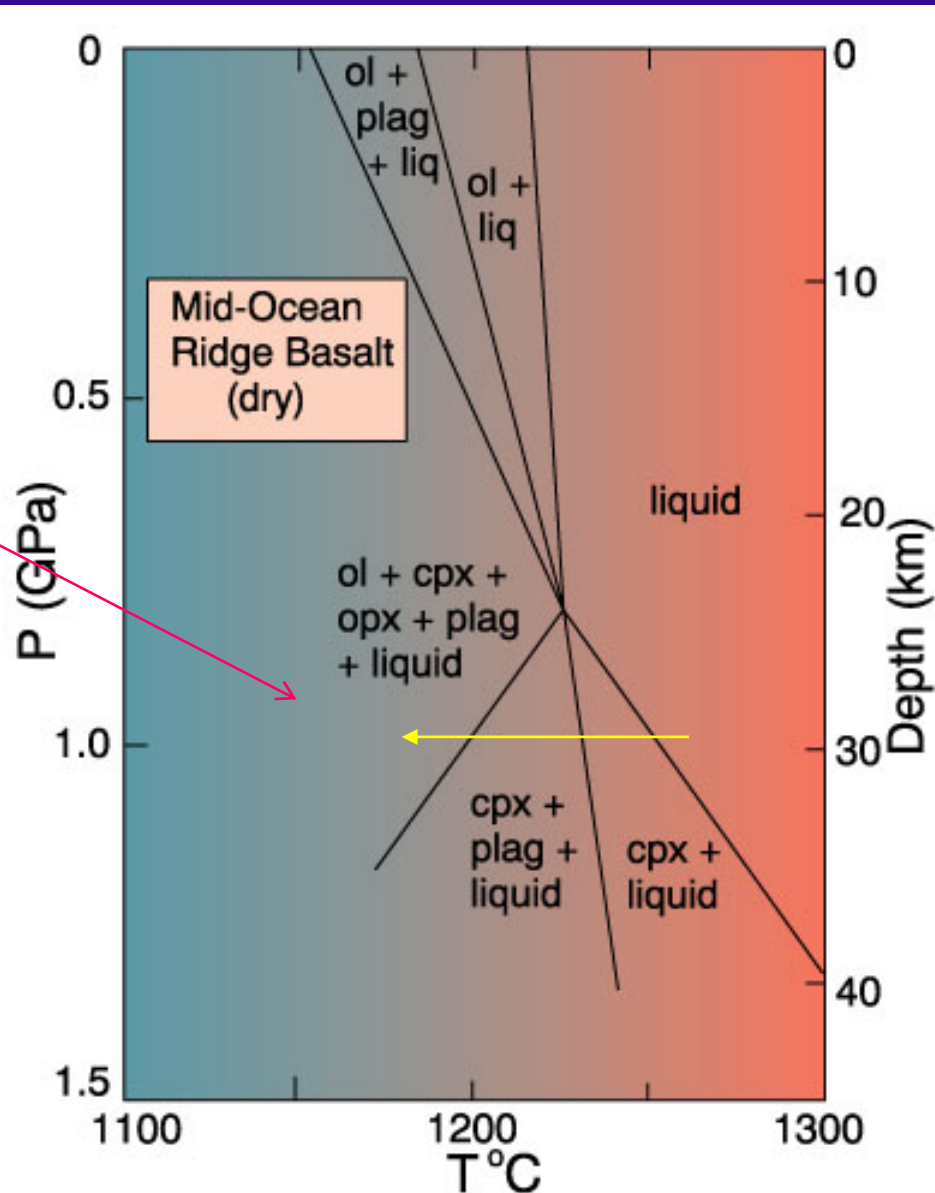


Multiple saturation with several mineral phases

At High P

- ◆ Cpx then Plag then Ol

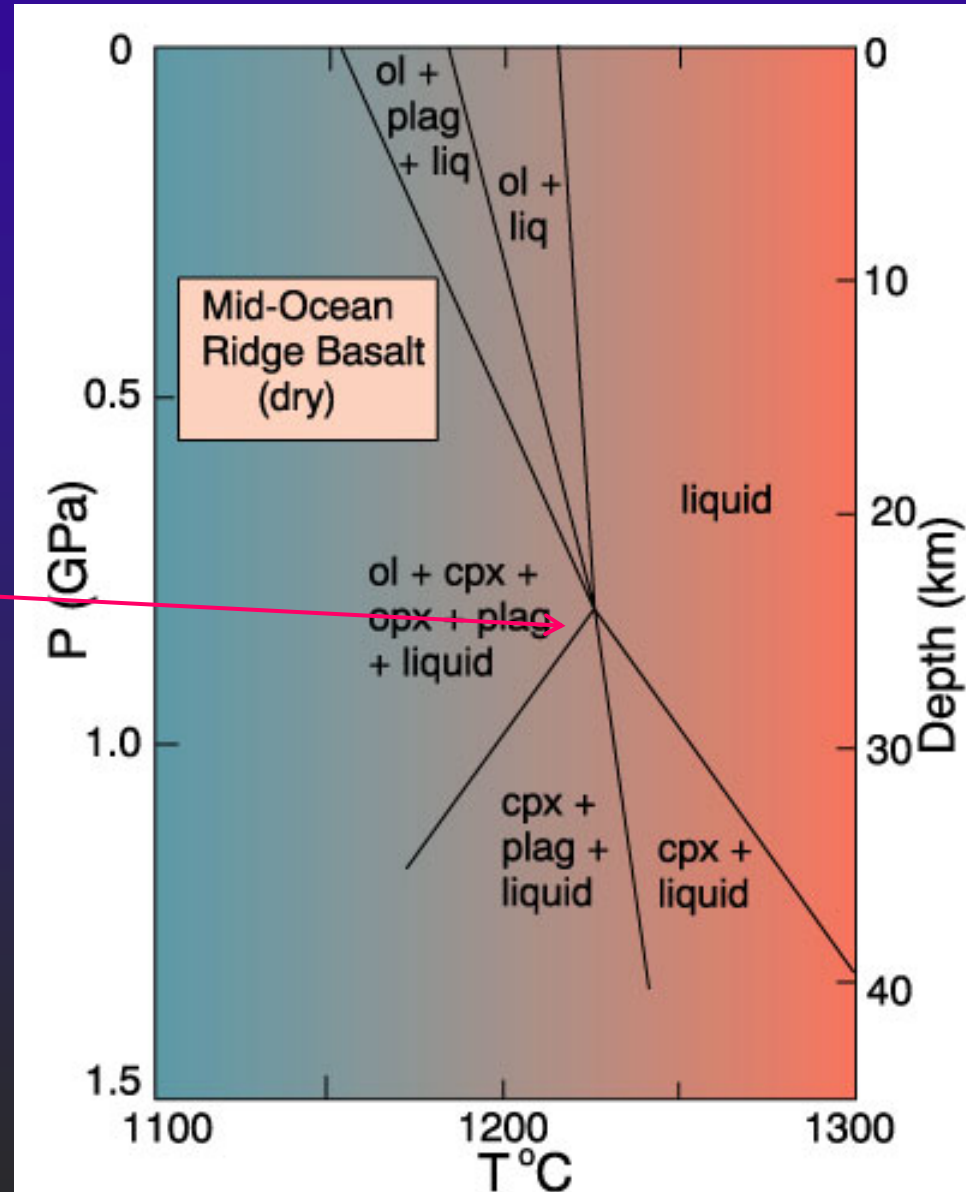
Figure 10-12 Anhydrous P-T phase relationships for a mid-ocean ridge basalt suspected of being a primary magma. After Fujii and Kushiro (1977). *Carnegie Inst. Wash. Yearb.*, 76, 461-465.



Multiple saturation with several mineral phases

At 25 km get all at once

- ◆ = Multiple saturation
- ◆ Suggests that 25 km is the depth of last equilibrium with the mantle



Summary

- A chemically homogeneous mantle can yield a variety of basalt types
- Alkaline basalts are favored over tholeiites by deeper melting and by low % PM
- Fractionation at moderate to high depths can also create alkaline basalts from tholeiites

Chemically Heterogeneous Mantle Model

Mantle Xenoliths – fragment of the mantle incorporated into a magma

Fertile xenoliths –

- higher in Ca, Al, Ti, Na and K
- lower in $\text{Mg}/(\text{Mg}+\text{Fe})$ and $\text{Cr}/(\text{Cr}+\text{Al})$

Depleted xenoliths – opposite of above

Trace element patterns –

REE (rare earth elements) are trace elements used to understand magma genesis

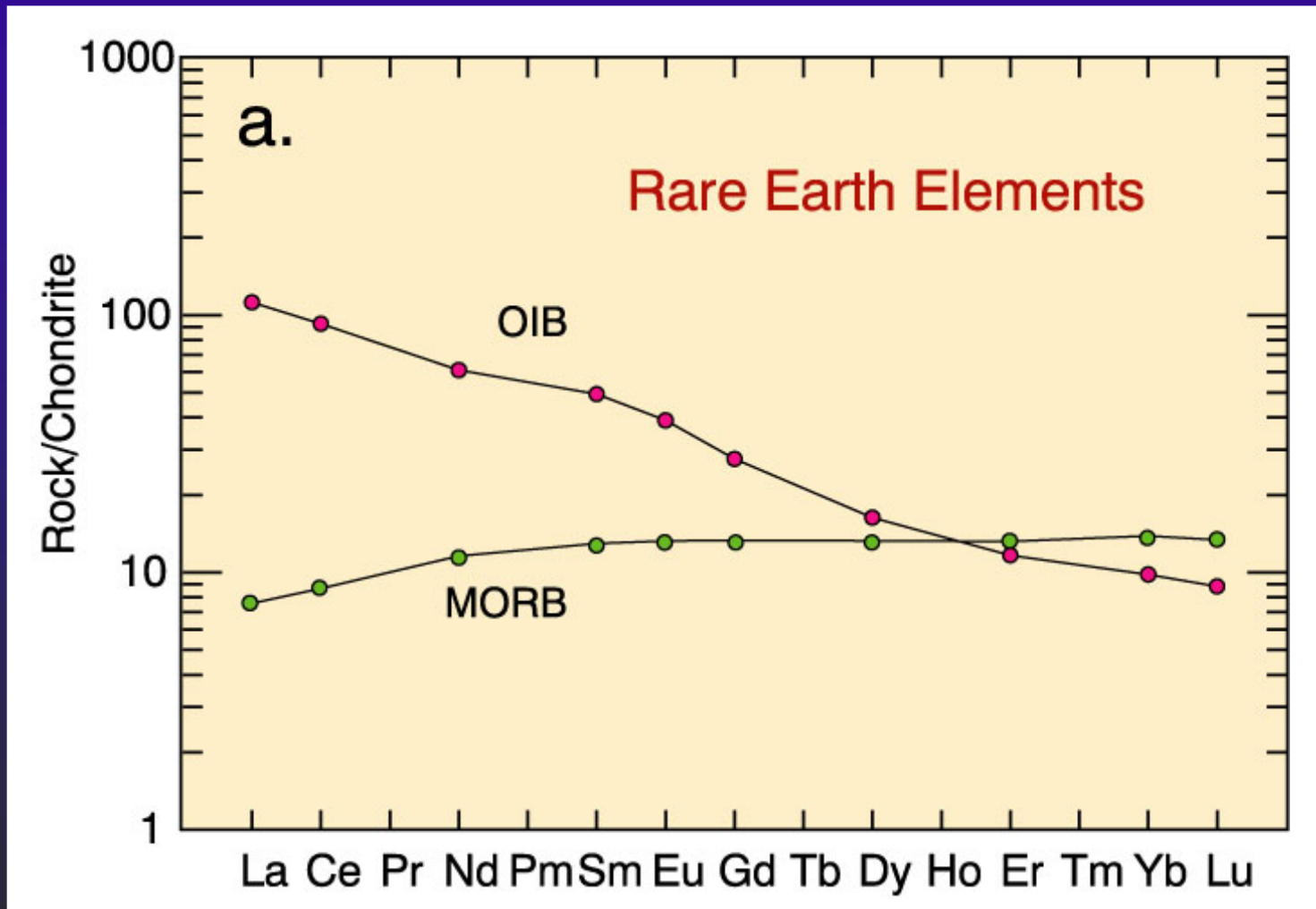
REE patterns for basalts show the following:

- MORB (mid-ocean ridge basalts) – most common magma; derived from depleted mantle from earlier extraction of oceanic and continental crust

- OIB (oceanic island basalts) – appear to have been derived from non-depleted (fertile) mantle sources

Conclusion: mantle not homogeneous; contains at least two principal reservoirs, depleted and fertile

REE data for oceanic basalt – different for OIB and MORB



← increasing incompatibility

Figure 10-13a. REE diagram for a typical alkaline ocean island basalt (OIB) and tholeiitic mid-ocean ridge basalt (MORB). From Winter (2001) *An Introduction to Igneous and Metamorphic Petrology*. Prentice Hall. Data from Sun and McDonough (1989).

REE data for ultramafic xenoliths from spinel and garnet lherzolite

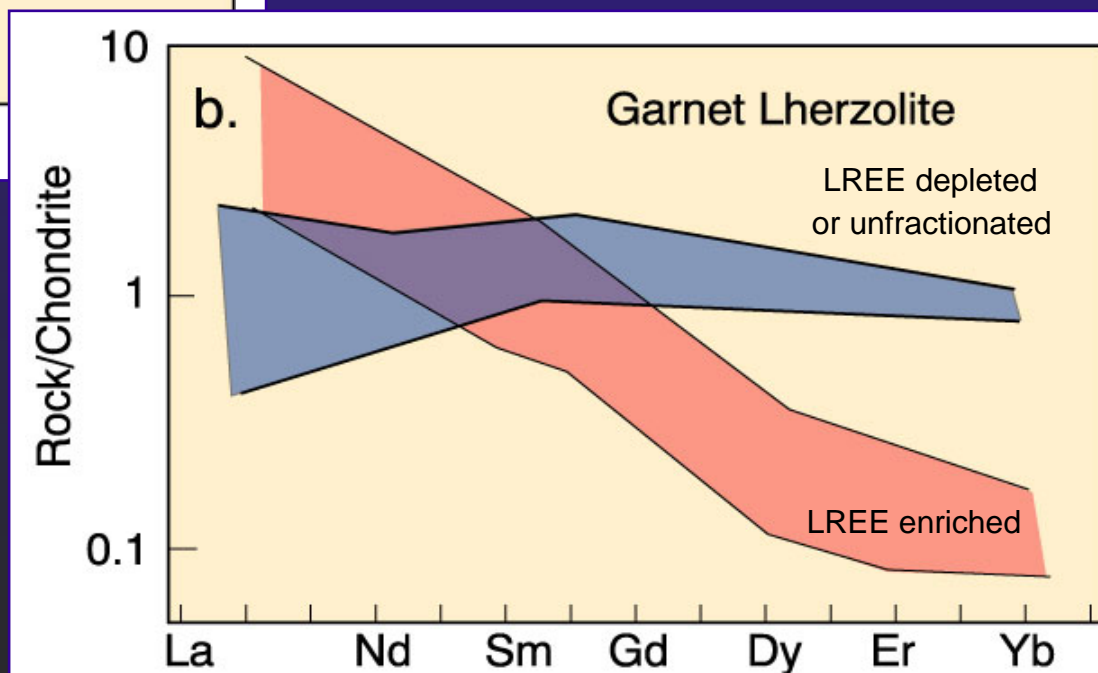
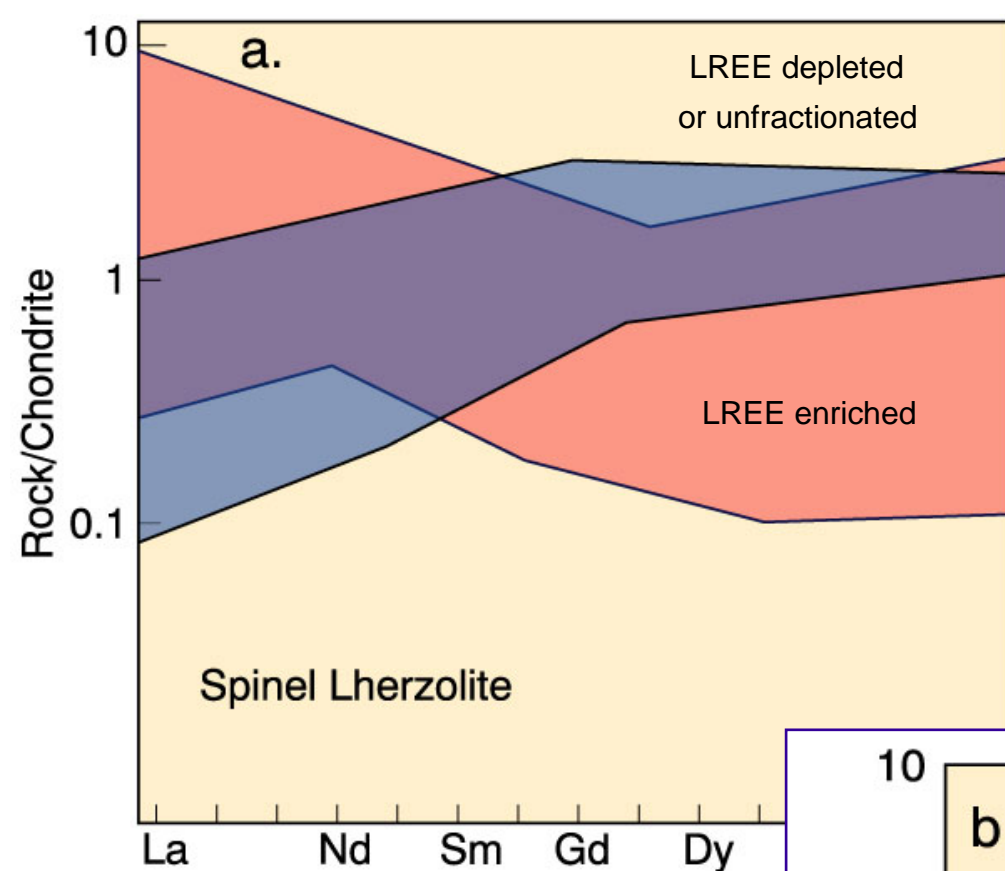
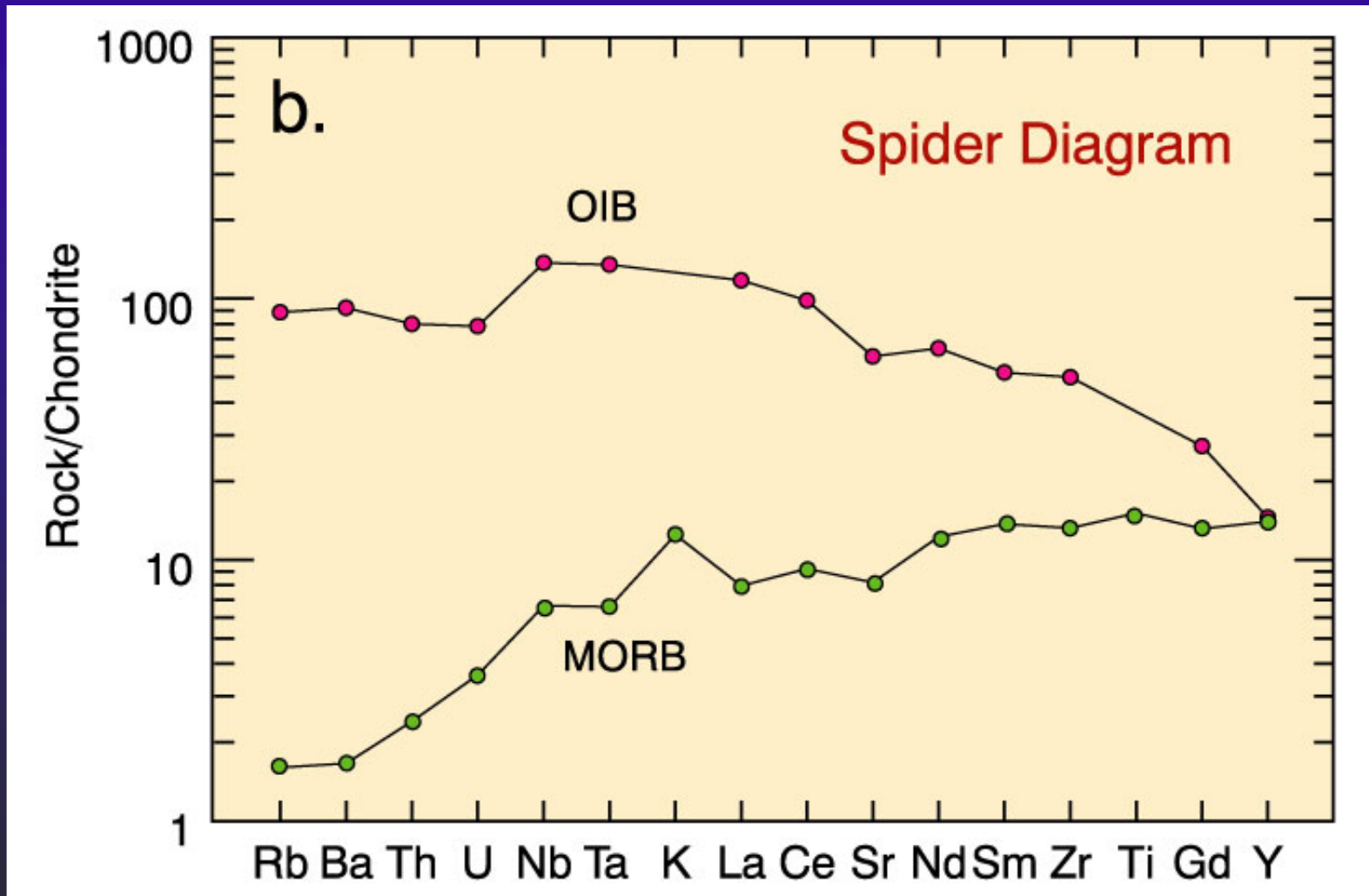


Figure 10-14 Chondrite-normalized REE diagrams for spinel (a) and garnet (b) lherzolites. After Basaltic Volcanism Study Project (1981). Lunar and Planetary Institute.

Spider diagram for OIB and MORB



← increasing incompatibility

Figure 10-13b. Spider diagram for a typical alkaline ocean island basalt (OIB) and tholeiitic mid-ocean ridge basalt (MORB). From Winter (2001) *An Introduction to Igneous and Metamorphic Petrology*. Prentice Hall. Data from Sun and McDonough (1989).

Sr Isotopic Evidence

^{87}Rb decays to ^{87}Sr $\lambda = 1.42 \times 10^{-11}$ yrs

Rb (parent) concentrated in enriched reservoir (continental crust) – considered incompatible

Enriched reservoir develops more ^{87}Sr (daughter) over time

Depleted reservoir (mantle - less Rb) - develops less ^{87}Sr over time

Review of Sr isotopes

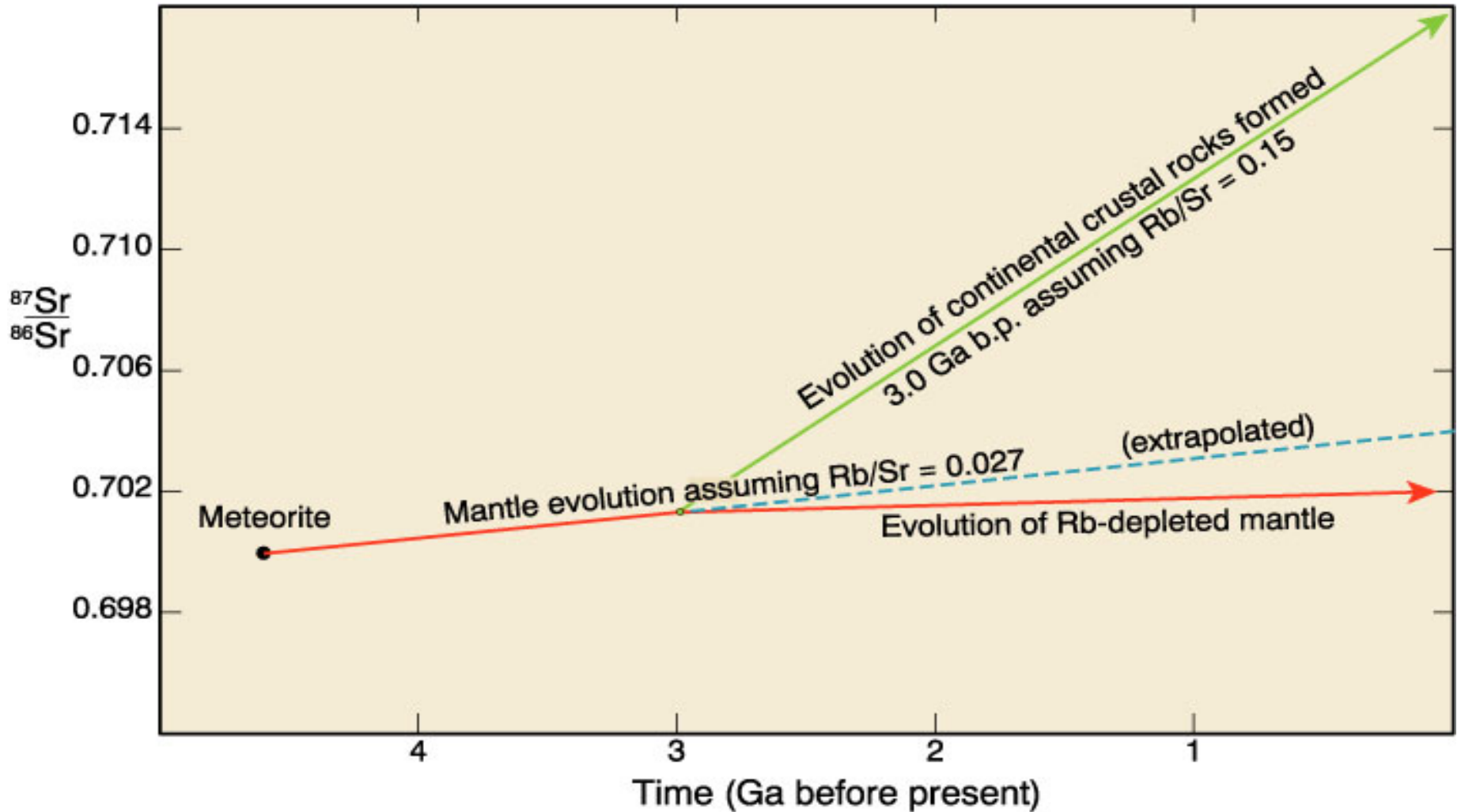
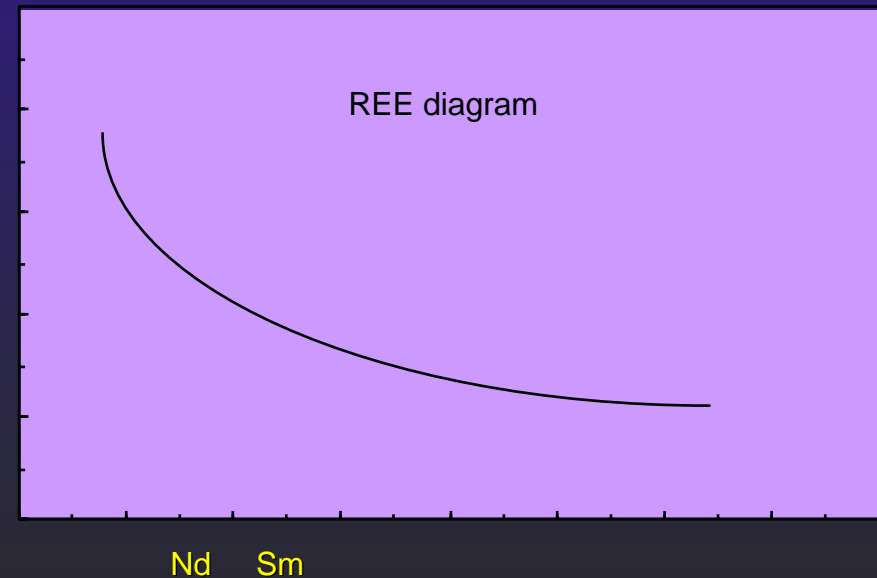


Figure 9-13. After Wilson (1989). *Igneous Petrogenesis*. Unwin Hyman/Kluwer.

Review of Nd isotopes

- $^{147}\text{Sm} \rightarrow ^{143}\text{Nd}$ $\lambda = 6.54 \times 10^{-13}$ yrs
- Nd (daughter) \rightarrow enriched reservoir (continental crust)
> Sm (parent)
Enriched reservoir develops less ^{143}Nd over time

Depleted reservoir (mantle)
(higher Sm/Nd) develops
higher
 $^{143}\text{Nd}/^{144}\text{Nd}$ over time



Nd Isotope Evolution

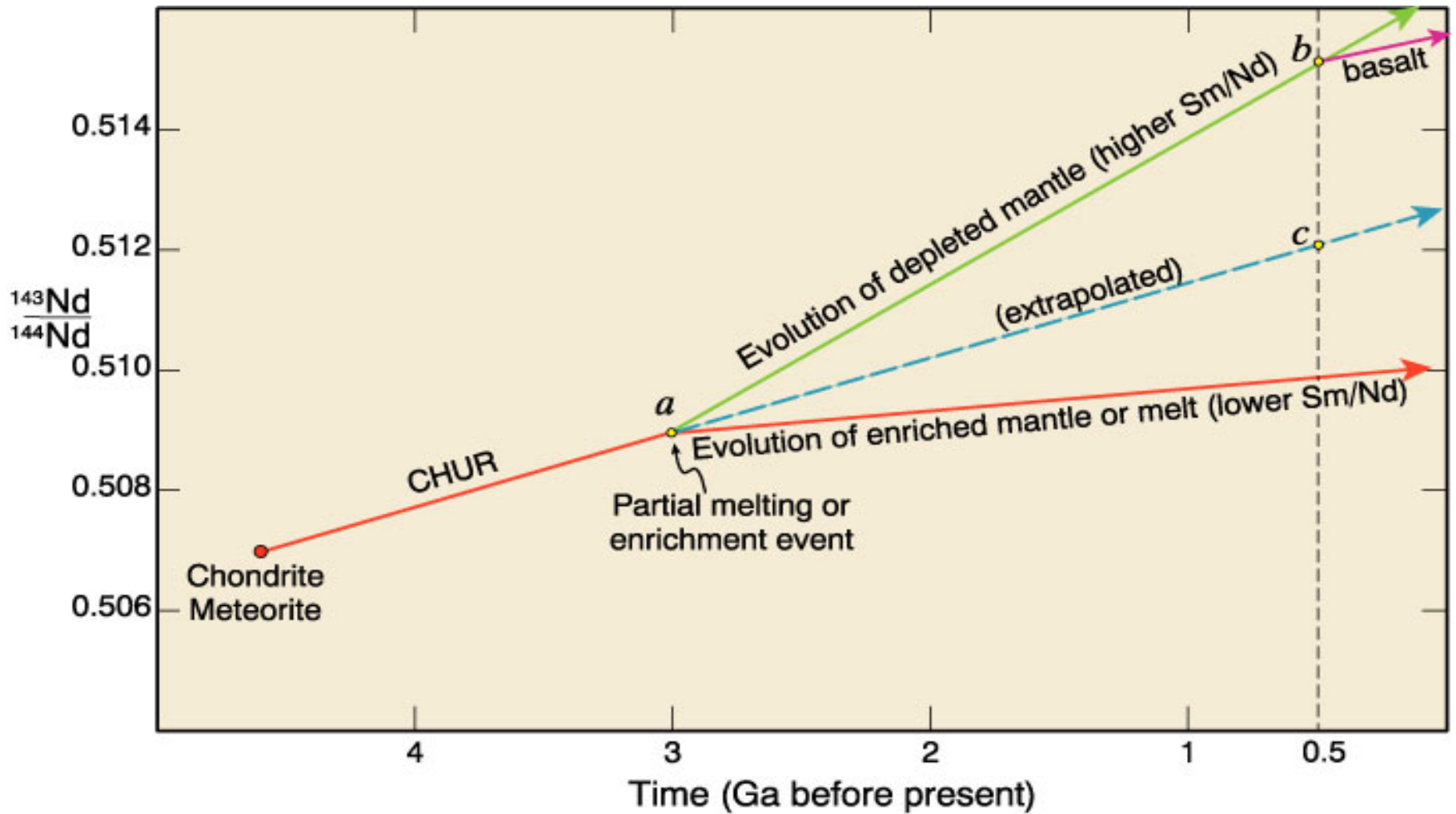


Figure 9-15. After Wilson (1989). Igneous Petrogenesis. Unwin Hyman/Kluwer

Nd and Sr isotopes of Ocean Basalts

“Mantle Array”

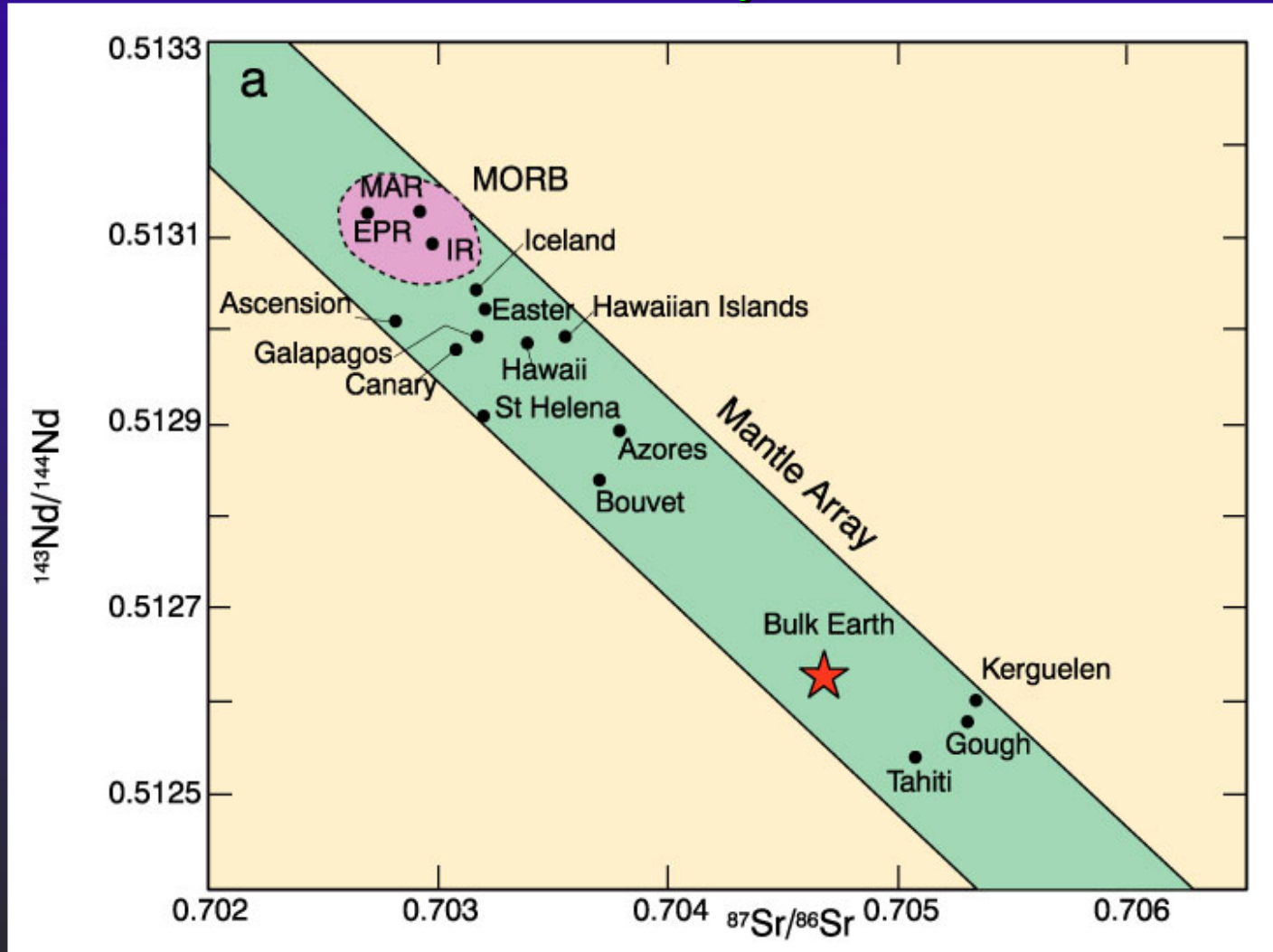


Figure 10-15 (a) Initial $^{143}\text{Nd}/^{144}\text{Nd}$ vs. $^{87}\text{Sr}/^{86}\text{Sr}$ for oceanic basalts. From Wilson (1989). *Igneous Petrogenesis*. Unwin Hyman/Kluwer. Data from Zindler *et al.* (1982) and Menzies (1983).

Whole Mantle Convection Model (1975)

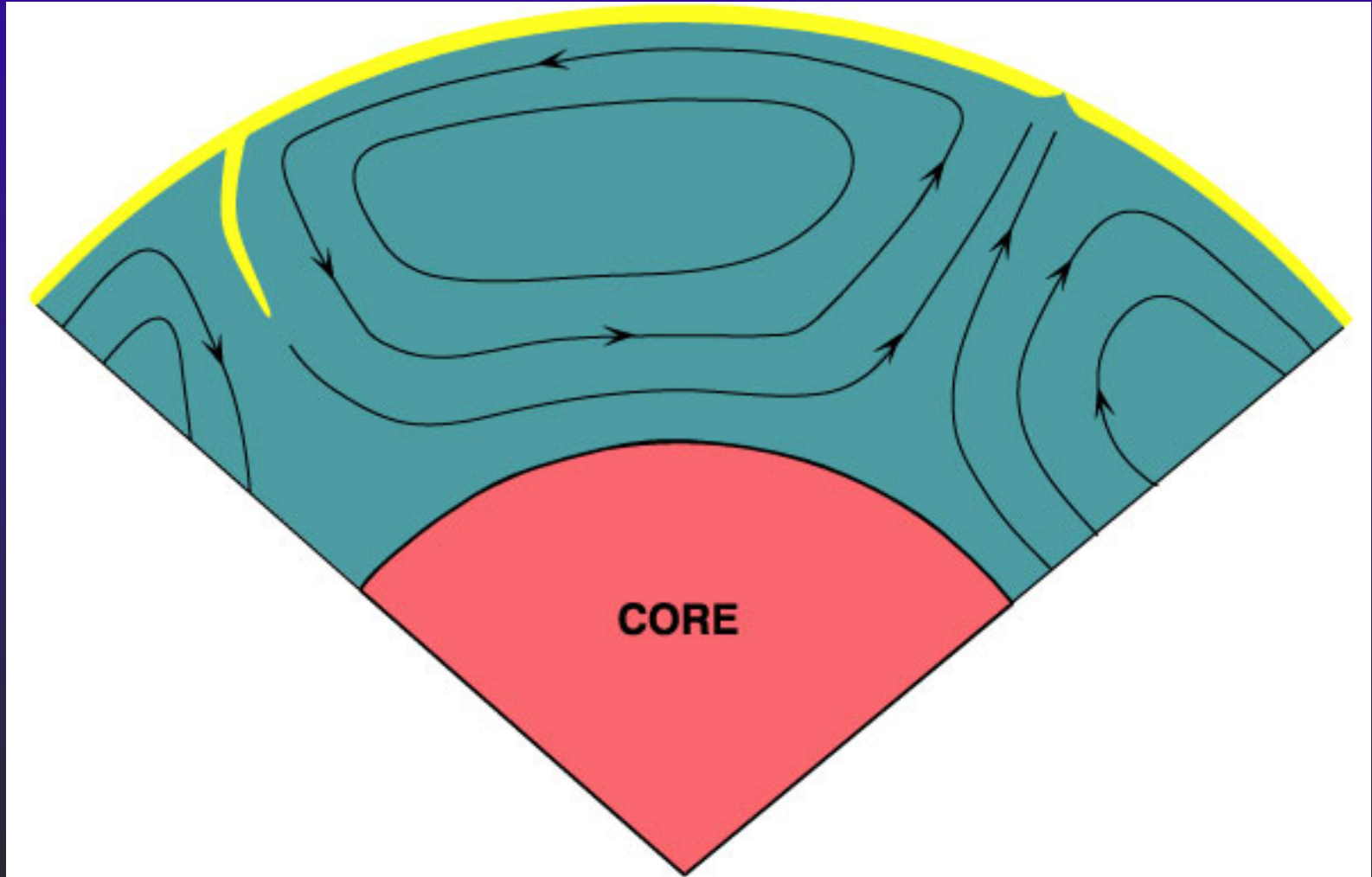


Figure 10-16a After Basaltic Volcanism Study Project (1981). Lunar and Planetary Institute.

Newer mantle convection model

- ✦ Upper depleted mantle = MORB source
- ✦ Lower undepleted and enriched OIB source

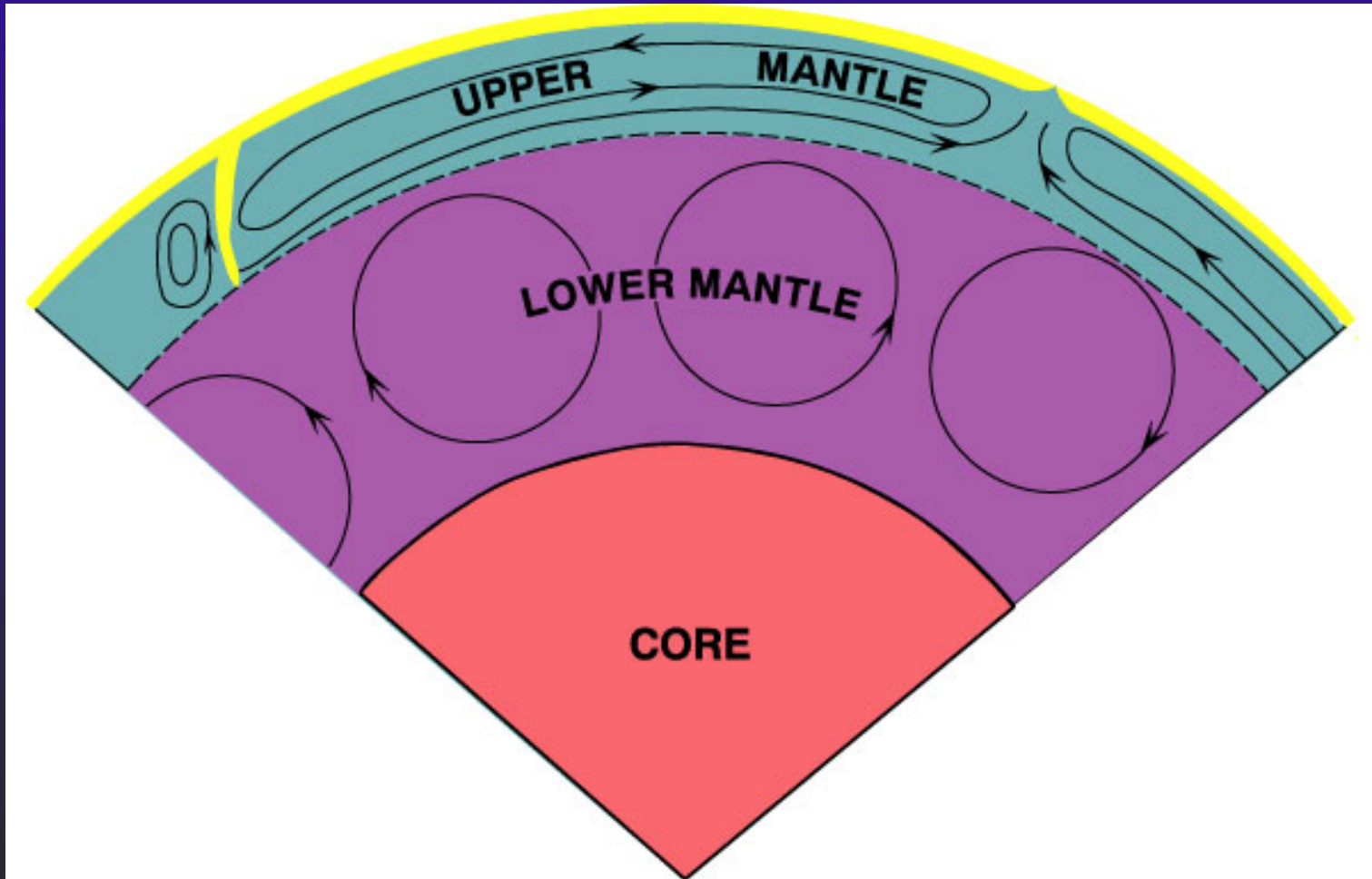


Figure 10-16b After Basaltic Volcanism Study Project (1981). Lunar and Planetary Institute.